Dehydroalkylative Activation of CNN- and PNN-Pincer Ruthenium Catalysts for Ester Hydrogenation

Tianyi He, John C. Buttner, Eamon F. Reynolds, John Pham, Jack C. Malek, Jason M. Keith,* and Anthony R. Chianese*

Department of Chemistry, Colgate University, 13 Oak Drive, Hamilton, NY 13346

ABSTRACT: Ruthenium-pincer complexes bearing CNN- and PNN-pincer ligands with diethyl- or diisopropylamino side groups, which have previously been reported to be active precatalysts for ester hydrogenation, undergo dehydroalkylation on heating in the presence of tricyclohexylphosphine to release ethane or propane, giving five-coordinate ruthenium(0) complexes containing a nascent imine functional group. Ethane or propane are also released under the conditions of catalytic ester hydrogenation, and time-course studies show that this release is concomitant with the onset of catalysis. A new PNN-pincer ruthenium(0)-imine complex is a highly active catalyst for ester hydrogenation at room temperature, giving up to 15,500 turnovers with no added base. This complex was shown to react reversibly at room temperature with two equivalents of hydrogen to give a ruthenium(II)-dihydride complex, where the imine functionality has been hydrogenated to give a protic amine side group. These observations have potentially broad implications for the identities of catalytic intermediates in ester hydrogenation and related transformations.

Introduction

Classical methods for the reduction of esters involve the use of stoichiometric hydride reagents that produce inorganic by-products and have low atom economy. Catalytic hydrogenation offers a more sustainable approach, especially at the industrial scale. The development of practically useful catalysts for ester hydrogenation was spurred by Milstein's 2006 report of the ruthenium-pincer complex **RuPNN^{dearom}**, formed by reaction of the hydridochloride precursor **RuPNN^{HCl}** with KO^{t}Bu (Equation 1).[1] Using **RuPNN^{dearom}**, several esters were cleanly hydrogenated to full conversion at 115 °C with up to 100 catalytic turnovers. The same complex is active for the microscopic reverse reaction, the acceptorless dehydrogenative coupling (ADC) of primary alcohols to give esters.[2] **RuPNN^{dearom}** was subsequently demonstrated to catalyze several mechanistically analogous reactions including amine-alcohol coupling,[3] couplings of amines[4] or alcohols[5] with esters, organic carbonate hydrogenation,[6] carbon dioxide hydrogenation,[7] and amide α-alkylation with alcohols.[8] More distantly related transformations including light-induced oxygen evolution,[9] alkene isomerization,[10] oxa-Michael addition,[11] and reduction of alkyl and aryl halides[12] were also reported to be catalyzed efficiently by **RuPNN^{dearom}**, either used directly or generated in situ by reaction of **RuPNN^{HCl}** with a strong base.

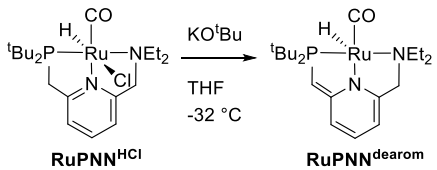

(1) **RuPNN^{HCl}** → **RuPNN^{dearom}**

In the intervening years, significant improvements in activity for ester hydrogenation have been achieved by many research groups through systematic modification of the catalyst structure. Chart 1 shows a selection of the most highly active catalysts for ester hydrogenation reported to date.[13] Almost all of the known "elite" catalyst systems feature an N-H functional group or anionic nitrogen donor reminiscent of Noyori's ruthenium catalysts for asymmetric ketone and imine hydrogenation;[14] a notable exception is Zhou's RuPNNN catalyst.[13d] For the Firmenich Ru(PN)$_2$,[13a] the Gusev RuSNS,[13c] and the Pidko RuCNC[13e] catalysts, the N-H group was demonstrated to be essential for high catalytic activity through the synthesis of control ligands where N-H was replaced with N-Me, N-Bn, or O. The highly beneficial effect of the N-H group has been taken as evidence that it is intimately involved in the catalytic mechanism, either through protonation/deprotonation of nitrogen during the catalytic cycle or by acting as a hydrogen-bond donor. Density functional theory analyses have provided support for this involvement in many cases.[13c, 13f, 13h, 13i, 15]

Chart 1. A selection of highly active catalysts for ester hydrogenation.

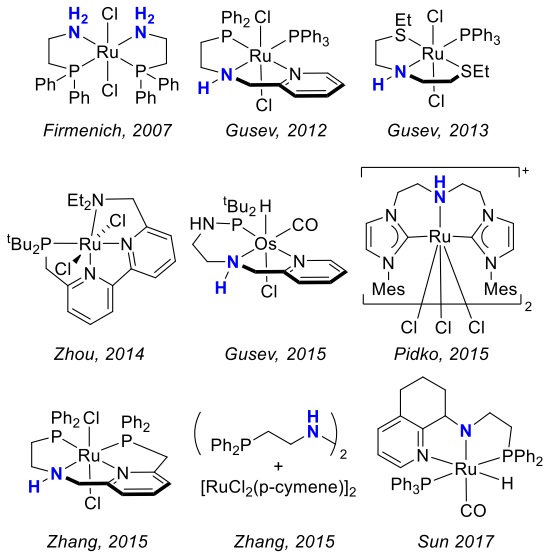

An interesting subclass of ester-hydrogenation catalysts features ligands with a dialkylamino side group, but no N-H functionality (Chart 2). This subclass includes the original Milstein catalyst **RuPNN^{dearom}**,[1] RuCNN complexes reported by Sánchez,[16] Song,[17] us,[18] and Zhou's RuPNNN catalyst.[13d]

Chart 2. Catalysts for ester hydrogenation featuring a dialkylamino group.

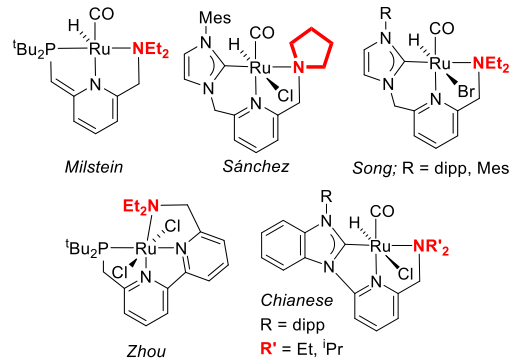

In their 2006 paper, Milstein and co-workers reported that **RuPNN^{dearom}** reversibly activates H_2 to form the re-aromatized dihydride complex **RuPNN^{H2}** (Equation 2). The NR_2 group appeared essential for ester hydrogenation catalysis, as analogous RuPNP complexes were significantly less active. Based on these observations, they proposed a mechanism for ester hydrogenation that involves heterolytic splitting of H_2 by **RuPNN^{dearom}** to form **RuPNN^{H2}**, followed by dechelation of the NEt_2 arm and inner-sphere transfer of hydrogen to the substrate.[1]

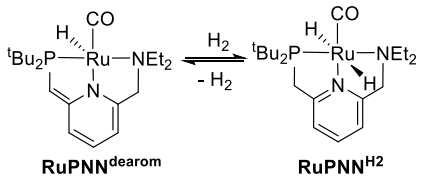

(2)

Much computational effort has been dedicated to understanding the mechanisms of reactions catalyzed by **RuPNN^{dearom}**.[19] In particular, catalytic oxygen evolution,[20] amide formation,[21] and carbonate hydrogenation[22] have received the most attention, although ester hydrogenation or its microscopic reverse, ADC, have been studied as well. In a DFT study by Wang focusing on the selectivity for **RuPNN^{dearom}** to catalyze amide formation over ester formation under dehydrogenative conditions, mechanisms involving metal-ligand cooperativity (MLC) were identified for both substrate dehydrogenation and H_2 release from **RuPNN^{H2}**, and a pathway involving dechelation of the NEt_2 group was excluded.[21a] Since this study reports a complete minimum-energy pathway for ADC, it is possible to apply the analysis to the microscopic reverse, ester hydrogenation. In this case, an application of the of the energetic span model[23] for the minimum-energy pathway reported by Wang predicts a high overall free-energy barrier of 38.5 kcal/mol for ester hydrogenation catalyzed by **RuPNN^{dearom}**, which would be consistent with it being largely *inactive* under the experimental catalytic conditions. More recently, Zhang has reported a DFT study directly focusing on ester hydrogenation by **RuPNN^{dearom}**.[24] Again, an MLC pathway involving reversible deprotonation of the CH_2 linker between phosphorus and the pyridine ring was identified, although in this case a more experimentally viable overall free-energy barrier of 27.2 kcal/mol was calculated. Interestingly, Hasanayn has identified a very different non-cooperative pathway for the reduction of esters by **RuPNN^{H2}**, consisting of a direct H/OR metathesis with no metal-ligand cooperativity.[25] Two additional studies consider the conversion of alcohols to aldehydes[26] or ketones[27] instead of esters. Detailed mechanistic analyses have not yet been reported for the other catalyst systems shown in Chart 2.

In attempting to characterize the stoichiometric reactivity of our RuCNN precatalysts under conditions relevant to ester hydrogenation, we recently observed that our RuCNN hydridochloride catalyst precursors rearranged to a CC binding mode upon reaction with NaO^{t}Bu and tertiary phosphines, resulting from dissociation of the dialkylamino group and C-H activation of the pyridine ring (Equation 3).[28] The RuCC complexes were also active catalysts for ester hydrogenation without the need for added base. Interestingly, the ligand structure-activity relationship was the same for the CNN[18b] and CC[28] forms of the precatalysts: in both cases, NMe_2-substituted variants were poorly active while NEt_2 and N^iPr_2 variants were highly active. This suggested that the CNN and CC forms may operate through a common catalytic pathway. We established through DFT that a reversion from the CC to the CNN binding mode is kinetically and thermodynamically viable under the catalytic conditions.[28]

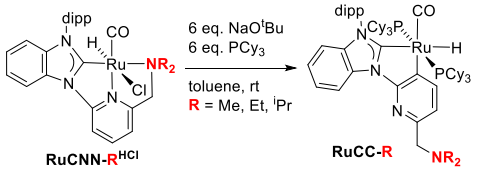

(3)

Further studies of the stoichiometric reactivity of our RuCC catalyst precursors uncovered a surprising result:

when the NEt_2 or N^iPr_2 variants are simply heated in toluene, they react to form five-coordinate ruthenium(0) complexes with concomitant loss of ethane or propane, where the amine group has converted to an imine group (Scheme 1, below). Even more surprisingly, we observed that the Milstein catalyst **RuPNN^{dearom}** undergoes an analogous reaction when heated in the presence of PCy_3 (Scheme 2, below). The newly synthesized CNN and PNN-pincer ruthenium(0)-imine complexes are highly active catalysts for ester hydrogenation. Herein we present evidence that the dehydroalkylation reaction is a *prerequisite for catalytic activity*, which has profound implications for the catalytic mechanism.

Results and Discussion

Catalyst Dehydroalkylation Reactions. When solutions of **RuCC-Et** or **RuCC-^{i}Pr** were heated overnight in toluene at 105 °C, conversion to a new major product occurred. Through spectroscopic and crystallographic analysis, we identified the products as the dark green, 18-electron, 5-coordinate ruthenium(0) complexes **RuCNN-Et^{imine}** and **RuCNN-^{i}Pr^{imine}** (Scheme 1, left). The same products were formed if **RuCNN-Et^{HCl}** or **RuCNN-^{i}Pr^{HCl}** were heated with excess NaO^{t}Bu and a slight excess of PCy_3 (Scheme 1, right). As the RuCC complexes are synthesized by rearrangement of the CNN hydridochloride complexes,[28] the latter route is more efficient and was preferred to isolate usable quantities of the products.

Scheme 1. Synthesis of RuCNN-imine complexes by dehydroalkylation.

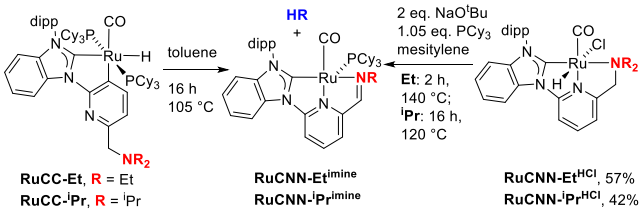

When a solution of **RuPNN^{dearom}** was heated to 100 °C for one hour in the presence of a slight excess of PCy_3, the analogous dehydroalkylation reaction was again observed, as the intensely purple product **RuPNN^{imine}** was formed cleanly (Scheme 2, left). **RuPNN^{imine}** could also be more conveniently synthesized from the thermally stable precursor **RuPNN^{HCl}** (Scheme 2, right), generating **RuPNN-^{dearom}** in situ with KO^{t}Bu. All three ruthenium(0)-imine complexes were observed to be highly air-sensitive, as their dark green or purple solutions decolorized nearly instantaneously upon exposure to air.

Scheme 2. Synthesis of RuPNN-imine complexes by dehydroalkylation.

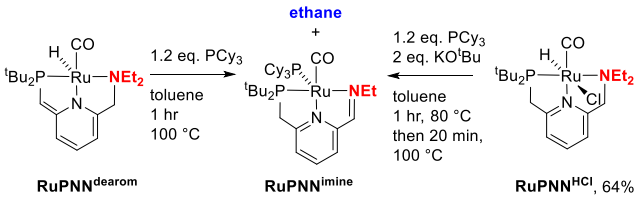

The formation of the ruthenium(0)-imine complexes requires the formal loss of an equivalent of ethane (**RuCC-Et** and **RuPNN^{dearom}**) or propane (**RuCC-^{i}Pr**). When these reactions were conducted in toluene-d_8 in sealed NMR tubes, the actual products were indeed confirmed to be ethane and propane, as identified by ^{1}H NMR, ^{13}C NMR, and HSQC.

The NMR spectra of **RuCNN-Et^{imine}**, **RuCNN-^{i}Pr^{imine}**, and **RuPNN^{imine}** are consistent with the structures shown in Schemes 1 and 2. In particular, the new imine hydrogens appear at 7.53-8.08 ppm, in each case showing splitting only by the phosphorus atoms. To unequivocally confirm their structures, all three complexes were characterized by X-ray crystallography; their solid-state structures are shown in Figures 1-3. The three structures are closely analogous, with imine C=N bond lengths of 1.337 – 1.347 Å indicating a clear double-bond character, and with nearly equal C-C bond lengths in the pyridine ring consistent with an aromatic structure, as opposed to the alternation around the ring observed for **RuPNN^{dearom}**.[1] The geometries about ruthenium can be described as distorted square-pyramidal, where the carbonyl and pincer ligands form the base and PCy_3 binds at the apex. The τ parameter[29] is 0.24 for **RuCNN-Et^{imine}** and **RuPNN^{imine}**, and 0.22 for **RuCNN-^{i}Pr^{imine}**, consistent with a structure closer to square-pyramidal than trigonal bipyramidal.

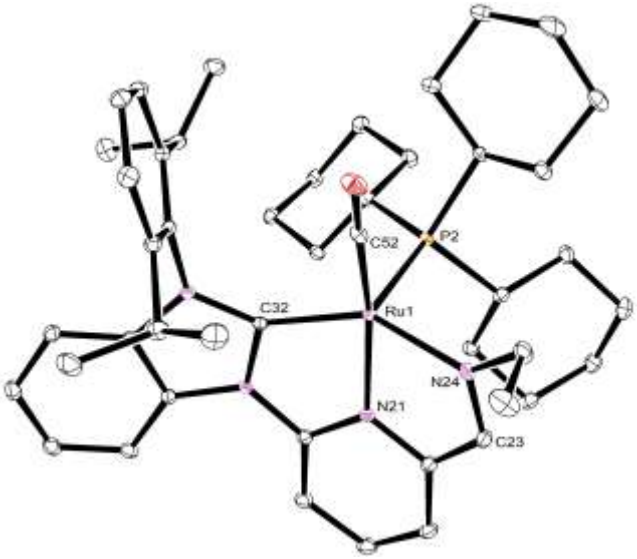

Figure 1. X-ray crystal structure of **RuCNN-Et^{imine}**, showing 50% probability ellipsoids. Hydrogen atoms have been omitted for clarity. Selected bond lengths (Å) and angles (°): Ru(1)–C(32), 1.9844(13); Ru(1)–N(21), 2.0041(11); Ru(1)–N(24), 2.0569(11); Ru(1)–P(2), 2.3315(3); Ru(1)–C(52), 1.8578(14); C(23)–N(24), 1.3451(18); C(32)–Ru(1)–N(21), 77.27(5); N(21)–Ru(1)–N(24), 76.34(5).

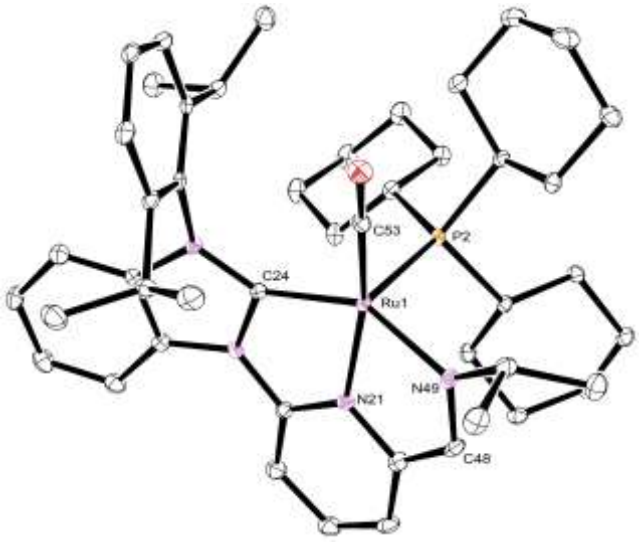

Figure 2. X-ray crystal structure of **RuCNN-^{i}Pr^{imine}**, showing 50% probability ellipsoids. Hydrogen atoms have been omitted for clarity. Selected bond lengths (Å) and angles (°): Ru(1)–C(24), 1.970(3); Ru(1)–N(21), 1.994(3); Ru(1)–N(49), 2.067(3); Ru(1)–P(2), 2.3493(9); Ru(1)–C(53), 1.857(3); C(48)–N(49), 1.346(5); C(24)–Ru(1)–N(21), 77.30(13); N(21)–Ru(1)–N(49), 76.28(12).

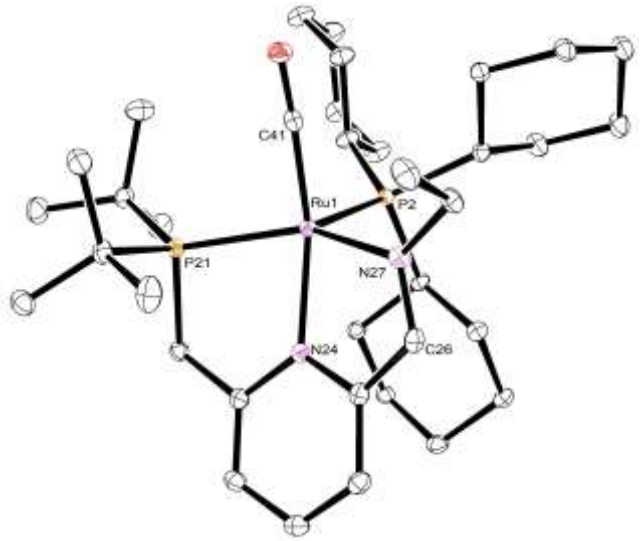

Figure 3. X-ray crystal structure of **RuPNN^{imine}**, showing 50% probability ellipsoids. Hydrogen atoms have been omitted for clarity. Selected bond lengths (Å) and angles (°): Ru(1)–P(21), 2.3221(6); Ru(1)–N(24), 2.0686(18); Ru(1)–N(27), 2.0527(19); Ru(1)–P(2), 2.3575(6); Ru(1)–C(41), 1.841(2); C(26)–N(27), 1.336(3); P(21)–Ru(1)–N(24), 79.18(5); N(24)–Ru(1)–N(27), 76.58(7).

We previously reported that the NMe_2-substituted catalyst variants **RuCC-Me** and **RuCNN-Me^{HCl}** were almost completely inactive as catalysts for ester hydrogenation.[28] Intriguingly, attempts to convert these catalytically inactive NMe_2 derivatives to ruthenium(0)-imine complexes analogous to those described above were unsuccessful: decomposition to an intractable mixture was observed, with no evidence of the analogous imine complex or methane observed by ^{1}H NMR (Scheme 3).

Scheme 3. No dehydroalkylation is observed for an NMe_2-substituted derivative.

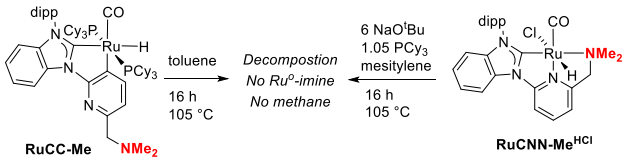

Ester Hydrogenation: Comparison of Amine and Imine Precatalyst Forms. In preliminary testing, we found that the new complexes **RuCNN-Et^{imine}**, **RuCNN-^{i}Pr^{imine}**, and **RuPNN^{imine}** were active catalysts for ester hydrogenation, without the need for added base. Since these imine-pincer complexes are formed by dehydroalkylation from amine-pincer complexes that are known catalysts for ester hydrogenation,[1, 28] we hypothesized that the dehydroalkylation reaction might be a *necessary* step in catalyst activation. We began assessing this possibility by conducting comparative hydrogenation experiments side-by-side under the same conditions (toluene, 20 bar H_2, 0.125 M hexyl hexanoate, 0.5% catalyst). Side-by-side monitoring was most conveniently conducted at 105 °C for the **CNN-Et** and **CNN-^{i}Pr** catalysts, and at 85 °C for the **PNN** catalysts. In addition to measuring the conversion of hexyl hexanoate into 1-hexanol over time, we monitored the headspace by gas chromatography to observe the formation of ethane or propane throughout the experiment.

Figure 4 shows the time course comparisons for the **CNN-Et**, **CNN-^{i}Pr**, and **PNN** catalysts. In each case, the ruthenium(0)-imine derivative is at least as active as its ruthenium(II)-amine precursor. The graphs on the left show the comparison of **RuCNN-Et^{imine}** with **RuCC-Et**. While **RuCC-Et** shows a moderate induction period before the onset of catalysis, **RuCNN-Et^{imine}** is active nearly from the start of the reaction. The middle graphs show the comparison of **RuCNN-^{i}Pr^{imine}** with **RuCC-^{i}Pr**, which convert hexyl hexanoate at nearly identical rates. The rightmost graphs show the comparison of **RuPNN^{dearom}** with **RuPNN^{imine}**. While **RuPNN^{dearom}** shows a long induction period before the onset of catalysis, **RuPNN^{imine}** is active at the very beginning of the reaction, and hydrogenation is 99% complete within 20 minutes.

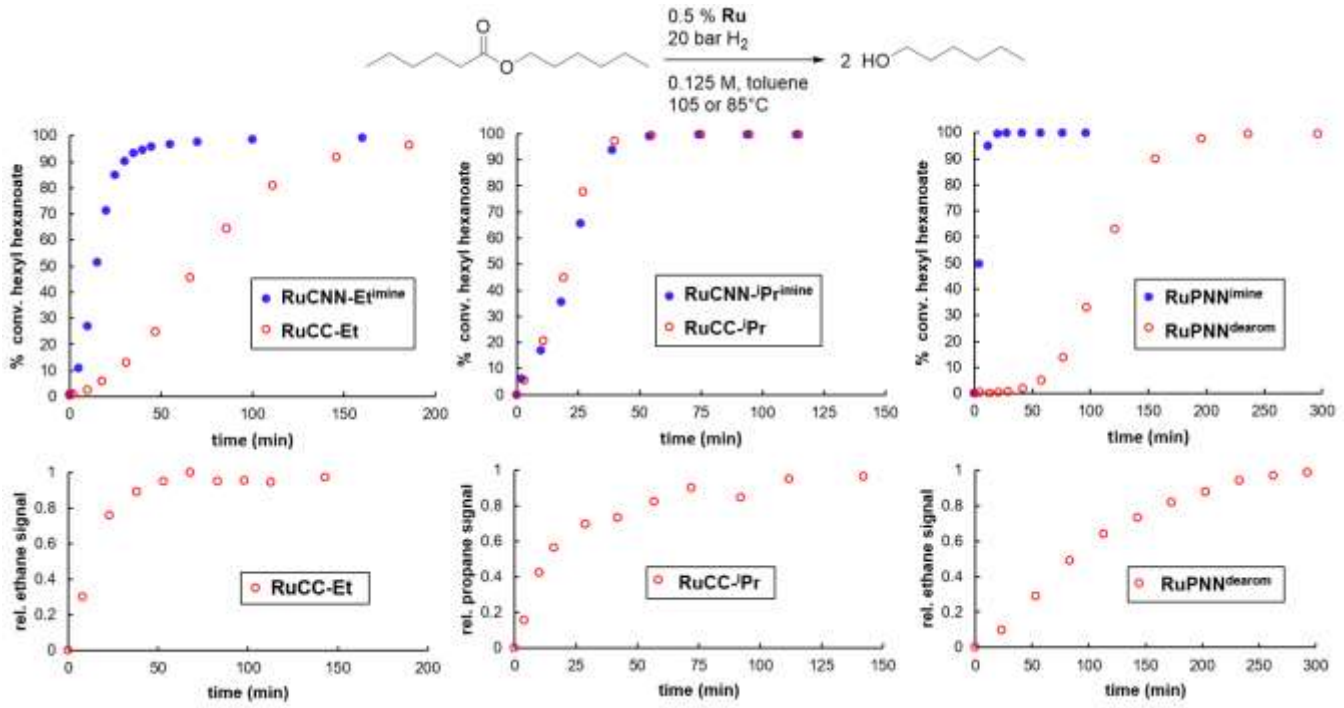

Figure 4. Ester hydrogenation time course comparisons for three ruthenium(0)-imine catalysts (filled circles) vs. their ruthenium(II)-amine precursors (open circles). The top graphs show the conversion of hexyl hexanoate over time, and the bottom graphs show the evolution of alkane in the headspace of reactions catalyzed by the ruthenium(II)-amine complexes. Reactions with CNN or CC ligands were conducted at 105 °C, while reactions with PNN ligands were conducted at 85 °C.

The lower graphs in Figure 4 show the formation of ethane from **RuCC-Et** or **RuPNN^{dearom}**, and propane from **RuCC-^{i}Pr**, as monitored over the course of each catalytic experiment. **RuCC-Et** and **RuCC-^{i}Pr** lose alkane rapidly at the start of the reaction, consistent with the short induction periods observed for these catalysts.[30] **RuPNN^{dearom}** releases ethane more slowly, consistent with the longer induction period observed under the conditions employed. No ethane or propane was produced in reactions catalyzed by any of the ruthenium(0)-imine forms, indicating that further loss of the second alkyl group does not occur in reactions catalyzed by the ruthenium(0)-imine complexes. No propane was produced when **RuCC-Et** or **RuPNN^{dearom}** were used and no ethane was produced when **RuCC-^{i}Pr** was used: this observation confirms that the observed ethane and propane come from the ligand dealkylation reaction, rather than some other, unidentified source.

These results, taken together, are consistent with the hypothesis that the dialkylamine variants of all three complexes represent precatalysts that must first undergo dehydroalkylation to generate the active catalyst, while the imine variants, having already undergone dehydroalkylation, can enter the catalytic cycle more rapidly (**RuCNN-Et^{imine}** and **RuPNN^{imine}**) or at a similar rate (**RuCNN-^{i}Pr^{imine}**).

Optimization and Substrate Scope for RuPNN^{imine}. Perhaps the most practically significant result of the above experiments is the observation that **RuPNN^{imine}** is an exceedingly active base-free catalyst for ester hydrogenation. In Milstein's original report,[1] a range of esters was hydrogenated using 1 mol % **RuPNN^{dearom}** at 115 °C in 1,4-dioxane under 5.3 atm H_2, with reaction times ranging from 4 to 24 hours. In our above comparisons, **RuPNN^{imine}** catalyzed the hydrogenation of hexyl hexanoate to 99% conversion in 20 minutes at 85 °C in toluene, with 0.5% catalyst loading and 30 bar H_2. Encouraged by the high rate of reaction at 85 °C, we conducted a screen of solvents at room temperature, with a higher, more practically useful 1.0 M substrate concentration and a lower 0.1 mol % catalyst loading (Figure 5). Ester hydrogenation did not occur appreciably in acetonitrile, and proceeded at a moderate rate in THF and toluene. Gratifyingly, the reaction proceeded to completion in isopropyl alcohol in five hours. The identification of a catalyst that operates efficiently under neutral conditions at room temperature is unique. Several catalyst systems have been reported to be active for hydrogenation of a broad range of ester substrates at[13d, 31] or near[13b, 13c, 15a, 32] room temperature, but the use of alkoxide base as co-catalyst has typically been necessary. On the other hand, many catalyst systems have been developed that operate without the need for added base,[1, 15g, 33] but elevated (≥80 °C) temperatures have been required for efficient conversion.

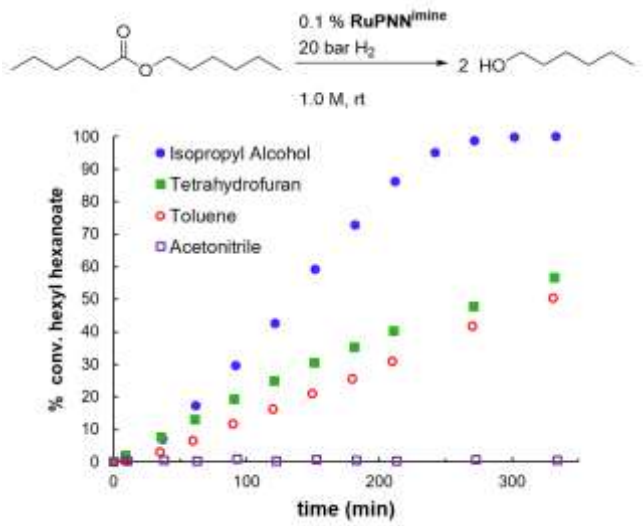

Figure 5. Comparison of solvents for room-temperature hydrogenation of hexyl hexanoate catalyzed by **RuPNN^{imine}**.

With the identification of optimal reaction conditions, we proceeded to survey the substrate scope (Table 1). **RuPNN^{imine}** is a highly effective catalyst for the hydrogenation of a range of aliphatic and aromatic esters (Entries 1-8), giving turnover numbers up to 15,500 (Entry 6). The hydrogenation of α-chiral esters without racemization is challenging: Kuriyama has reported an effective base-free ruthenium catalyst system for this transformation,[33a] and Clarke has successfully employed the weak base K_2CO_3 to minimize racemization in a manganese-catalyzed transformation.[34] Using our optimized conditions, (*S*)-ethyl ibuprofen was hydrogenated effectively, but a small amount of racemization was observed, as the alcohol product had only 97% ee (Entry 9). The chemoselective hydrogenation of esters in the presence of other reducible functional groups such as alkenes is also an important goal, and some catalyst systems have been reported to offer such selectivity.[13f, 15j, 32c, 35] Under our optimized conditions, an ester was hydrogenated completely with nearly perfect selectivity in the presence of an internal alkene (Entry 10). When a substrate containing a terminal alkene was employed (Entry 11), we observed complete ester hydrogenation accompanied by 14% alkene hydrogenation at 0.1% catalyst loading, and a lower 83% yield at 0.05% loading, albeit with only 1% hydrogenation of the double bond. Thus, **RuPNN^{imine}** was highly selective against the hydrogenation of an internal alkene, and moderately selective against the hydrogenation of a terminal alkene.

Table 1. Substrate Scope for Ester Hydrogenation Catalyzed by RuPNN^{imine}

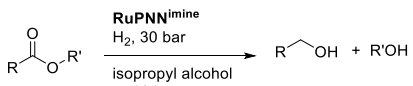

Entry	Substrate	[Sub] /[Ru]	% Yield
1	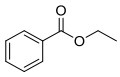	8,000 16,000	99 83
2	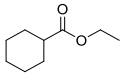	4,000	92
3		8,000	95
4	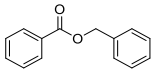	8,000 16,000	99 83
5		1,000	94
6	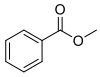	16,000	97
7		8,000	98
8		8,000	94
9[a]	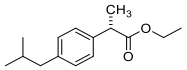	2,000	98, 97% ee
10[b]	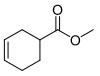	8,000	96, 99.9% sel
11[b]	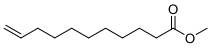	1,000 2,000	99, 86% sel 83, 99% sel

[a]The reactant (*S*)-ethyl ibuprofen had >99% ee, as determined by GC. [b]Yields given represent the sum of all alkene and alkane alcohol products from ester hydrogenation. Reported % selectivities represent the percentage of product resulting from no hydrogenation or isomerization of the C=C bond.

Reaction of RuPNN^{imine} with Hydrogen. The high catalytic activity of **RuPNN^{imine}** for ester hydrogenation at room temperature prompted us to examine its reaction with hydrogen. When a dilute (0.2 mM) solution of **RuPNN^{imine}** in toluene-d_8 was placed under 10 bar hydrogen, complete conversion to a nearly colorless product occurred in approximately 20 minutes at room temperature (Equation 4). We have assigned the product as **RuPNN^{HEt}**, on the basis of its ^{1}H, ^{31}P, COSY, and NOESY spectra, informed by the close structural similarity to the previously reported[1] compound **RuPNN^{H2}** (Equation 2), which differs only by its amine substituents (NHEt vs NEt_2), and the resulting loss of a time-averaged plane of symmetry. Removal of the solvent under vacuum resulted in complete reversion back to **RuPNN^{imine}**, indicating the reversibility of both the net oxidative addition to ruthenium(0) and the hydrogenation of the ligand's imine functionality at room temperature. Attempts to prepare a more concentrated sample for more

detailed spectroscopic analysis resulted in the formation of a second, unidentified product, complicating the analysis.

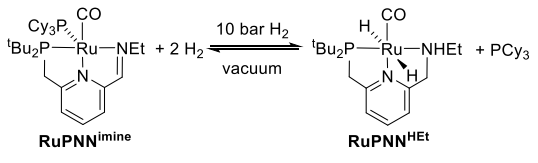

RuPNN^{imine} RuPNN^{HEt} (4)

The NMR spectra of **RuPNN^{HEt}** are broad at room temperature, and are sharpest at −30 °C. The Ru-bound phosphorus atom resonates at 120.6 ppm, and free PCy_3 is observed as expected. The two chemically inequivalent ruthenium-hydrides appear at −4.42 and −5.07 ppm, and show slightly different H-P coupling constants of 13.4 and 17.6 Hz, respectively. Linewidths of 5-6 Hz preclude measurement of the H-H coupling constant, which is expected to be small based on closely analogous compounds.[36] The broad N-H resonance appears at 4.13 ppm at 22 °C and 5.77 ppm at −30 °C. (See the Supporting Information for ^{1}H NMR spectra taken from -70 °C to 60 °C.)

Thermodynamic Analysis by DFT. As an additional validation of the structural assignment of **RuPNN^{HEt}**, we have computed the thermodynamics of the reaction shown in Equation 4 using density functional theory. To assess whether the analogous double hydrogenation reaction is thermodynamically feasible for the N-heterocyclic carbene derivatives, we also analyzed the analogous reaction of **RuCNN-Et^{imine}** to give **RuCNN^{HEt}**, which we have not yet studied experimentally. Scheme 4 shows the calculated standard-state free energies for these transformations, calculated at the B3LYP-D3/6-311G(d,p)/LANL08(f)//M06/6-311G(d,p)/LANL08(f) level of theory. The hydrogenation of **RuPNN^{imine}** to release PCy_3 and give **RuPNN^{HEt}** is calculated to be endergonic by only 0.1 kcal/mol, consistent with the observation that the reaction is reversible at room temperature. Similarly, the analogous hydrogenation of **RuCNN-Et^{imine}** is endergonic by only 0.8 kcal/mol.

Scheme 4. Relative standard-state free energies at 298.15 K for ruthenium(0)-imine complexes and their doubly hydrogenated derivatives. Energies are given in kcal/mol.

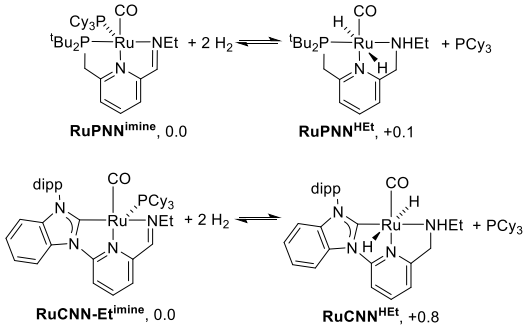

Implications for the Catalytic Mechanism. Several lines of evidence support the hypothesis that ruthenium precatalysts based on NR_2-substituted CNN- and PNN-pincer ligands are not significantly active catalysts for ester hydrogenation prior to the occurrence of the dehydroalkylation reactions described above: 1) three different ruthenium(0)-imine complexes formed via dehydroalkylation were shown to be kinetically competent catalysts, leading to either the same catalytic rate as their ruthenium(II)-amine precursor (**RuCC-^{i}Pr**) or showing a shorter induction period (**RuCC-Et** and **RuPNN^{dearom}**); 2) Reactions catalyzed by the ruthenium(II)-amine precursors showed release of ethane or propane, concomitant with the onset of catalysis; and 3) an analogous NMe_2-substituted variant of our **RuCC** precatalysts is nearly inactive for ester hydrogenation,[28] and also does not undergo dehydroalkylation to form a ruthenium(0)-imine complex.

The facile formation of **RuPNN^{HEt}** from **RuPNN^{imine}** (Equation 4) raises the intriguing possibility that **RuPNN^{HEt}** is an on- or off-cycle intermediate in catalytic ester hydrogenation. Although we have not yet experimentally characterized the reactivity of **RuCNN-Et^{imine}** and **RuCNN-^{i}Pr^{imine}** with hydrogen, we have shown computationally that a doubly hydrogenated complex analogous to **RuPNN^{HEt}** is thermodynamically accessible for the NHC-based **RuCNN-Et^{imine}** as well. We noted in the introduction the overwhelming preponderance of the N-H functional group in the most highly active catalysts for ester hydrogenation (Chart 1). In the extensive computational literature on ester hydrogenation,[13c, 13f, 13h, 13i, 15] a common theme involves the heterolytic cleavage of H_2 by its addition to a ruthenium-amido intermediate, followed by concerted or stepwise transfer of hydrogen to the substrate. Recently, Dub and Ikariya[15b] and Dub and Gordon[37] have demonstrated that a mechanism where the N-H group functions only as hydrogen-bond donor without being deprotonated as part of the catalytic cycle is energetically preferable in some cases. Such mechanisms involving N-H deprotonation or hydrogen-bond donation are clearly unavailable to the NR_2-substituted precatalysts shown in Chart 2, which lack the requisite N-H group. However, these mechanisms are possible if dehydroalkylation followed by hydrogenation can occur, as we have demonstrated for **RuPNN^{dearom}**. Our current working hypothesis is that many, if not all, of the NR_2-substituted precatalysts shown in Chart 2 may actually operate in ester hydrogenation by first losing an equivalent of alkane, then being hydrogenated to give an NHR-substituted derivative that serves as the actual catalyst, i.e. the NR_2 group may serve as a latent NHR group under catalytic conditions.

Broader Mechanistic Implications. Because **RuPNN^{dearom}** has been reported to be an active catalyst for a wide array of additional transformations, the possibility exists that catalyst dehydroalkylation occurs in more cases than the one presently discussed, and could potentially be a prerequisite for catalysis in other scenarios, especially when elevated temperatures are employed. Many dehydrogenative coupling reactions[3-5, 8] have been reported to be catalyzed by **RuPNN^{dearom}** or **RuPNN^{HCl}** activated in situ by base, all of which occur at temperatures greater than 100 °C where the dehydroalkylation might be expected to occur rapidly. Similarly, hydrogenation of dimethyl carbonate to methanol catalyzed by **RuPNN^{dearom}** occurs at 145 °C,[6] and hydrogenation of carbon dioxide to formate occurs at 120 °C.[7] In contrast, catalytic alkene isomerization[10] and oxa-Michael addition to nitriles[11] occur rapidly at room temperature, where dehydroalkylation is potentially slower.

Separately, it is noteworthy that Milstein and coworkers have identified the complex **RuPNNH^{tBu}** (Figure 6) as a highly active catalyst (in combination with base) for a variety of reactions, including ester hydrogenation and the reverse ADC reaction,[31] as well as related reactions with potential application in hydrogen storage.[38] This complex could conceivably undergo base-promoted dehydrochlorination followed by addition of H_2 to give a dihydride complex analogous to **RuPNN^{HEt}**. This raises the possibility that **RuPNNH^{tBu}** operates in a mechanistically analogous fashion to **RuPNN^{imine}** and **RuPNN^{dearom}**. The **PNNH^{tBu}** ligand has been applied in manganese[33i, 39] and cobalt[40] catalysis, where its NEt_2variant has been substantially less active. De Bruin and coworkers have synthesized a related rhodium complex of a PNNH-type pincer ligand, and demonstrated dynamic ligand reactivity including the stepwise dehydrogenation of the amine group to an imine.[41] Related PNN pincer ligands containing the imine functionality have been applied in a variety of hydrogenations and hydrosilylations.[42] The observation of reversible ligand hydrogenation (Equation 4) suggests that hydrogenation or hydrosilylation of the imine functionality may be plausible in these systems as well.

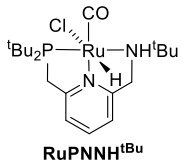

RuPNNH^{tBu}

Figure 6. Ruthenium-pincer complex containing an N-H group reported by Milstein.

Mechanistic Hypotheses for Catalyst Dehydroalkylation. The dehydroalkylation reactions shown in Schemes 1 and 2 are unexpected, and we are actively interrogating their mechanisms in a combined experimental and computational study. Although we are unable to make conclusions at this time, our hypotheses draw on the observed reactivity of ethyl and isopropyl groups and the lack of reactivity of methyl groups. Plausible mechanisms include: 1) β-CH-activation followed by β-amido elimination,[43] then hydrogenation of the resulting alkene; 2) a Cope-elimination-like[44] direct transfer of the β-hydrogen to the benzylic position, again releasing the alkene which can subsequently be hydrogenated; and 3) homolytic N-C bond cleavage to release an ethyl or 2-propyl radical, followed by hydrogen atom abstraction at the benzylic position. Another mechanism (4) involving direct transfer of the alkyl group from N to Ru seems less likely, as it is not obvious why the reaction would not occur for the NMe_2 variant.

Conclusions

In summary, we report the observation of an unexpected ligand transformation, where ruthenium(II)-pincer complexes containing NEt_2 or N^iPr_2 groups undergo dehydroalkylation to give ruthenium(0)-pincer complexes containing an imine functionality, with loss of ethane or propane. We have demonstrated that the resulting ruthenium(0)-imine complexes are active catalysts for ester hydrogenation, and experiments are consistent with the hypothesis that the dehydroalkylation is a *prerequisite* for catalytic activity in these systems. The observed double hydrogenation of **RuPNN^{imine}** to give **RuPNN^{HEt}** suggests that a catalytic mechanism involving the N-H functional group may be operative in ester hydrogenation and related transformations. Additionally, we have demonstrated that **RuPNN^{imine}** is one of the most highly active catalysts for base-free ester hydrogenation reported to date, giving in excess of 15,000 turnovers at room temperature with no added base. Experimental and computational studies to understand the mechanisms of ligand dealkylation, double hydrogen addition to the resulting ruthenium(0)-imine complexes, and catalytic ester hydrogenation are underway.

Associated Content

Supporting Information

The Supporting Information is available free of charge on the ACS Publications website at DOI:xxx.

Experimental procedures, images of NMR spectra and detailed NMR assignments for new compounds, and computational details (PDF). Crystallographic details (CIF). Atomic coordinates for all computed molecular structures, compiled as one file readable by the free program Mercury[45] (XYZ).

Author Information

Corresponding Author

*E-mail: achianese@colgate.edu

Notes

The authors declare no competing financial interest.

Acknowledgements

We thank the National Science Foundation (CHE-1665144) for support of the research project, and (CHE-1726308) for the acquisition of an upgraded NMR spectrometer.

References

(1) Zhang, J.; Leitus, G.; Ben-David, Y.; Milstein, D. Efficient Homogeneous Catalytic Hydrogenation of Esters to Alcohols. *Angew. Chem. Int. Ed.* **2006,** *45*, 1113-1115.

(2) Zhang, J.; Leitus, G.; Ben-David, Y.; Milstein, D. Facile Conversion of Alcohols into Esters and Dihydrogen Catalyzed by New Ruthenium Complexes. *J. Am. Chem. Soc.* **2005,** *127*, 10840-10841.

(3) (a) Gunanathan, C.; Ben-David, Y.; Milstein, D. Direct Synthesis of Amides from Alcohols and Amines with Liberation of H_2. *Science* **2007,** *317*, 790-792. (b) Gnanaprakasam, B.; Balaraman, E.; Ben-David, Y.; Milstein, D. Synthesis of Peptides and Pyrazines from Beta-Amino Alcohols through Extrusion of H_2 Catalyzed by Ruthenium Pincer Complexes: Ligand-Controlled Selectivity. *Angew. Chem. Int. Ed.* **2011,** *50*, 12240-12244. (c) Zeng, H.; Guan, Z. Direct Synthesis of Polyamides Via Catalytic Dehydrogenation of Diols and Diamines. *J. Am. Chem. Soc.* **2011,** *133*, 1159-1161. (d) Rigoli, J. W.; Moyer, S. A.; Pearce, S. D.; Schomaker, J. M. Alpha,Beta-Unsaturated Imines Via Ru-Catalyzed Coupling of Allylic Alcohols and Amines. *Org. Biomol. Chem.* **2012,** *10*, 1746-1749.

(4) Gnanaprakasam, B.; Milstein, D. Synthesis of Amides from Esters and Amines with Liberation of H_2 under Neutral Conditions. *J. Am. Chem. Soc.* **2011,** *133*, 1682-1685.

(5) Gnanaprakasam, B.; Ben-David, Y.; Milstein, D. Ruthenium Pincer-Catalyzed Acylation of Alcohols Using Esters with Liberation of Hydrogen under Neutral Conditions. *Adv. Synth. Catal.* **2010,** *352*, 3169-3173.

(6) Balaraman, E.; Gunanathan, C.; Zhang, J.; Shimon, L. J. W.; Milstein, D. Efficient Hydrogenation of Organic Carbonates, Carbamates and Formates Indicates Alternative Routes to Methanol Based on CO_2 and CO. *Nature Chem.* **2011,** *3*, 609-614.

(7) Huff, C. A.; Sanford, M. S. Catalytic CO_2 Hydrogenation to Formate by a Ruthenium Pincer Complex. *ACS Catal.* **2013,** *3*, 2412-2416.

(8) Chaudhari, M. B.; Bisht, G. S.; Kumari, P.; Gnanaprakasam, B. Ruthenium-Catalyzed Direct Alpha-Alkylation of Amides Using Alcohols. *Org. Biomol. Chem.* **2016,** *14*, 9215-9220.

(9) Milstein, D.; Iron, M. A.; Ben-David, Y.; Shimon, L. J.; Konstantinovski, L.; Schwartsburd, L.; Weiner, L.; Kohl, S. W. Consecutive Thermal H_2 and Light-Induced O_2 Evolution from Water Promoted by a Metal Complex. *Science* **2009,** *324*, 74-77.

(10) Perdriau, S.; Chang, M. C.; Otten, E.; Heeres, H. J.; de Vries, J. G. Alkene Isomerisation Catalysed by a Ruthenium PNN Pincer Complex. *Chem. Eur. J.* **2014,** *20*, 15434-15442.

(11) Perdriau, S.; Zijlstra, D. S.; Heeres, H. J.; de Vries, J. G.; Otten, E. A Metal-Ligand Cooperative Pathway for Intermolecular Oxa-Michael Additions to Unsaturated Nitriles. *Angew. Chem. Int. Ed.* **2015,** *54*, 4236-40.

(12) Haibach, M. C.; Stoltz, B. M.; Grubbs, R. H. Catalytic Reduction of Alkyl and Aryl Bromides Using Propan-2-ol. *Angew. Chem. Int. Ed.* **2017,** *56*, 15123-15126.

(13) (a) Saudan, L. A.; Saudan, C. M.; Debieux, C.; Wyss, P. Dihydrogen Reduction of Carboxylic Esters to Alcohols under the Catalysis of Homogeneous Ruthenium Complexes: High Efficiency and Unprecedented Chemoselectivity. *Angew. Chem. Int. Ed.* **2007,** *46*, 7473-7476. (b) Spasyuk, D.; Gusev, D. G. Acceptorless Dehydrogenative Coupling of Ethanol and Hydrogenation of Esters and Imines. *Organometallics* **2012,** *31*, 5239-5242. (c) Spasyuk, D.; Smith, S.; Gusev, D. G. Replacing Phosphorus with Sulfur for the Efficient Hydrogenation of Esters. *Angew. Chem. Int. Ed.* **2013,** *52*, 2538-2542. (d) Li, W.; Xie, J.-H.; Yuan, M.-L.; Zhou, Q.-L. Ruthenium Complexes of Tetradentate Bipyridine Ligands: Highly Efficient Catalysts for the Hydrogenation of Carboxylic Esters and Lactones. *Green Chem.* **2014,** *16*, 4081-4085. (e) Filonenko, G. A.; Aguila, M. J. B.; Schulpen, E. N.; van Putten, R.; Wiecko, J.; Müller, C.; Lefort, L.; Hensen, E. J. M.; Pidko, E. A. Bis-N-Heterocyclic Carbene Aminopincer Ligands Enable High Activity in Ru-Catalyzed Ester Hydrogenation. *J. Am. Chem. Soc.* **2015,** *137*, 7620-7623. (f) Spasyuk, D.; Vicent, C.; Gusev, D. G. Chemoselective Hydrogenation of Carbonyl Compounds and Acceptorless Dehydrogenative Coupling of Alcohols. *J. Am. Chem. Soc.* **2015,** *137*, 3743-3746. (g) Tan, X.; Wang, Q.; Liu, Y.; Wang, F.; Lv, H.; Zhang, X. A New Designed Hydrazine Group-Containing Ruthenium Complex Used for Catalytic Hydrogenation of Esters. *Chem. Commun.* **2015,** *51*, 12193-12196. (h) Tan, X.; Wang, Y.; Liu, Y.; Wang, F.; Shi, L.; Lee, K. H.; Lin, Z.; Lv, H.; Zhang, X. Highly Efficient Tetradentate Ruthenium Catalyst for Ester Reduction: Especially for Hydrogenation of Fatty Acid Esters. *Org. Lett.* **2015,** *17*, 454-457. (i) Wang, Z.; Chen, X.; Liu, B.; Liu, Q.-B.; Solan, G. A.; Yang, X.; Sun, W.-H. Cooperative Interplay between a Flexible PNN-Ru(II) Complex and a $NaBH_4$ Additive in the Efficient Catalytic Hydrogenation of Esters. *Catal. Sci. Technol.* **2017,** *7*, 1297-1304.

(14) Noyori, R.; Ohkuma, T. Asymmetric Catalysis by Architectural and Functional Molecular Engineering: Practical Chemo- and Stereoselective Hydrogenation of Ketones. *Angew. Chem. Int. Ed.* **2001,** *40*, 40-73.

(15) (a) O, W. W. N.; Morris, R. H. Ester Hydrogenation Catalyzed by a Ruthenium(II) Complex Bearing an N-Heterocyclic Carbene Tethered with an "NH_2" Group and a DFT Study of the Proposed Bifunctional Mechanism. *ACS Catal.* **2013,** *3*, 32-40. (b) Otsuka, T.; Ishii, A.; Dub, P. A.; Ikariya, T. Practical Selective Hydrogenation of Alpha-Fluorinated Esters with Bifunctional Pincer-Type Ruthenium(II) Catalysts Leading to Fluorinated Alcohols or Fluoral Hemiacetals. *J. Am. Chem. Soc.* **2013,** *135*, 9600-9603. (c) Chakraborty, S.; Lagaditis, P. O.; Förster, M.; Bielinski, E. A.; Hazari, N.; Holthausen, M. C.; Jones, W. D.; Schneider, S. Well-Defined Iron Catalysts for the Acceptorless Reversible Dehydrogenation-Hydrogenation of Alcohols and Ketones. *ACS Catal.* **2014,** *4*, 3994-4003. (d) Chen, T.; Li, H.; Qu, S.; Zheng, B.; He, L.; Lai, Z.; Wang, Z.-X.; Huang, K.-W. Hydrogenation of Esters Catalyzed by Ruthenium PN_3-Pincer Complexes Containing an Aminophosphine Arm. *Organometallics* **2014,** *33*, 4152-4155. (e) Junge, K.; Wendt, B.; Jiao, H.; Beller, M. Iridium-Catalyzed Hydrogenation of Carboxylic Acid Esters. *ChemCatChem* **2014,** *6*, 2810-2814. (f) Qu, S.; Dai, H.; Dang, Y.; Song, C.; Wang, Z.-X.; Guan, H. Computational Mechanistic Study of Fe-Catalyzed Hydrogenation of Esters to Alcohols: Improving Catalysis by Accelerating Precatalyst Activation with a Lewis Base. *ACS Catal.* **2014,** *4*, 4377-4388. (g) Werkmeister, S.; Junge, K.; Wendt, B.; Alberico, E.; Jiao, H.; Baumann, W.; Junge, H.; Gallou, F.; Beller, M. Hydrogenation of Esters to Alcohols with a Well-Defined Iron Complex. *Angew. Chem. Int. Ed.* **2014,** *53*, 8722-8726. (h) Chen, X.; Jing, Y.; Yang, X. Unexpected Direct Hydride Transfer Mechanism for the Hydrogenation of Ethyl Acetate to Ethanol Catalyzed by SNS Pincer Ruthenium Complexes. *Chem. Eur. J.* **2016,** *22*, 1950-1957. (i) Gusev, D. G. Dehydrogenative Coupling of Ethanol and Ester Hydrogenation Catalyzed by Pincer-Type YNP Complexes. *ACS Catal.* **2016,** *6*, 6967-6981. (j) van Putten, R.; Uslamin, E. A.; Garbe, M.; Liu, C.; Gonzalez-de-Castro, A.; Lutz, M.; Junge, K.; Hensen, E. J. M.; Beller, M.; Lefort, L.; Pidko, E. A. Non-Pincer-Type Manganese Complexes as Efficient Catalysts for the Hydrogenation of Esters. *Angew. Chem. Int. Ed.* **2017,** *56*, 7531-7534.

(16) del Pozo, C.; Iglesias, M.; Sánchez, F. l. Pincer-Type Pyridine-Based N-Heterocyclic Carbene Amine Ru(II) Complexes as Efficient Catalysts for Hydrogen Transfer Reactions. *Organometallics* **2011,** *30*, 2180-2188.

(17) Sun, Y.; Koehler, C.; Tan, R.; Annibale, V. T.; Song, D. Ester Hydrogenation Catalyzed by Ru-CNN Pincer Complexes. *Chem. Commun.* **2011,** *47*, 8349-8351.

(18) (a) Kim, D.; Le, L.; Drance, M. J.; Jensen, K. H.; Bogdanovski, K.; Cervarich, T. N.; Barnard, M. G.; Pudalov, N. J.; Knapp, S. M. M.; Chianese, A. R. Ester Hydrogenation Catalyzed by CNN-Pincer Complexes of Ruthenium. *Organometallics* **2016,** *35*, 982-989. (b) Le, L.; Liu, J.; He, T.; Kim, D.; Lindley, E. J.; Cervarich, T. N.; Malek, J. C.; Pham, J.; Buck, M. R.; Chianese, A. R. Structure–Function Relationship in Ester Hydrogenation Catalyzed by Ruthenium CNN-Pincer Complexes. *Organometallics* **2018,** *37*, 3286-3297.

(19) Li, H.; Hall, M. B. Computational Mechanistic Studies on Reactions of Transition Metal Complexes with Noninnocent Pincer Ligands: Aromatization–Dearomatization or Not. *ACS Catal.* **2015,** *5*, 1895-1913.

(20) (a) Fang, W.-H.; Chen, Y. Mechanism for the Light-Induced O_2 Evolution from H_2o Promoted by Ru(II) PNN Complex: A DFT Study. *J. Phys. Chem. A* **2010,** *114*, 10334-10338. (b) Yang, X.; Hall, M. B. Mechanism of Water Splitting and Oxygen-Oxygen Bond Formation by a Mononuclear Ruthenium Complex. *J. Am. Chem. Soc.* **2010,** *132*, 120-130. (c) Sandhya, K. S.; Suresh, C. H. Water Splitting Promoted by a Ruthenium(II) PNN Complex: An Alternate Pathway through a Dihydrogen Complex for Hydrogen Production. *Organometallics* **2011,** *30*, 3888-3891. (d) Ma, C.; Piccinin, S.; Fabris, S. Reaction Mechanisms of Water Splitting and H_2 Evolution by a Ru(II)-Pincer Complex Identified with Ab Initio Metadynamics Simulations. *ACS Catal.* **2012,** *2*, 1500-1506. (e) Sandhya, K. S.; Remya, G. S.; Suresh, C. H. Pincer Ligand Modifications to Tune the Activation Barrier for H_2 Elimination in Water Splitting Milstein Catalyst. *Inorg Chem* **2015,** *54*, 11150-11156.

(21) (a) Li, H.; Wang, X.; Huang, F.; Lu, G.; Jiang, J.; Wang, Z.-X. Computational Study on the Catalytic Role of Pincer Ruthenium(II)-PNN Complex in Directly Synthesizing Amide

from Alcohol and Amine: The Origin of Selectivity of Amide over Ester and Imine. *Organometallics* **2011,** *30*, 5233-5247. (b) Zeng, G.; Li, S. Insights into Dehydrogenative Coupling of Alcohols and Amines Catalyzed by a (PNN)-Ru(II) Hydride Complex: Unusual Metal-Ligand Cooperation. *Inorg. Chem.* **2011,** *50*, 10572-10580. (c) Cho, D.; Ko, K. C.; Lee, J. Y. Catalytic Mechanism for the Ruthenium-Complex-Catalyzed Synthesis of Amides from Alcohols and Amines: A DFT Study. *Organometallics* **2013,** *32*, 4571-4576. (d) Hasanayn, F.; Harb, H. A Metathesis Model for the Dehydrogenative Coupling of Amines with Alcohols and Esters into Carboxamides by Milstein's [Ru(PNN)(CO)(H)] Catalysts. *Inorg. Chem.* **2014,** *53*, 8334-8349. (e) Li, L.; Lei, M.; Liu, L.; Xie, Y.; Schaefer, H. F. Metal-Substrate Cooperation Mechanism for Dehydrogenative Amidation Catalyzed by a PNN-Ru Catalyst. *Inorg. Chem.* **2018,** *57*, 8778-8787.

(22) (a) Li, H.; Wen, M.; Wang, Z.-X. Computational Mechanistic Study of the Hydrogenation of Carbonate to Methanol Catalyzed by the (RuPNN)-P-II Complex. *Inorg. Chem.* **2012,** *51*, 5716-5727. (b) Yang, X. Metal Hydride and Ligand Proton Transfer Mechanism for the Hydrogenation of Dimethyl Carbonate to Methanol Catalyzed by a Pincer Ruthenium Complex. *ACS Catal.* **2012,** *2*, 964-970. (c) Hasanayn, F.; Baroudi, A.; Bengali, A. A.; Goldman, A. S. Hydrogenation of Dimethyl Carbonate to Methanol by Trans-[$Ru(H)_2$(PNN)(CO)] Catalysts: DFT Evidence for Ion-Pair-Mediated Metathesis Paths for C–OMe Bond Cleavage. *Organometallics* **2013,** *32*, 6969-6985.

(23) Kozuch, S.; Shaik, S. How to Conceptualize Catalytic Cycles? The Energetic Span Model. *Acc. Chem. Res.* **2010,** *44*, 101-110.

(24) Wang, H.; Liu, C.; Zhang, D. Decisive Effects of Solvent and Substituent on the Reactivity of Ru-Catalyzed Hydrogenation of Ethyl Benzoate to Benzyl Alcohol and Ethanol: A DFT Study. *Mol. Catal.* **2017,** *440*, 120-132.

(25) Hasanayn, F.; Baroudi, A. Direct H/OR and OR/OR′ Metathesis Pathways in Ester Hydrogenation and Transesterification by Milstein's Catalyst. *Organometallics* **2013,** *32*, 2493-2496.

(26) Yang, X. A Self-Promotion Mechanism for Efficient Dehydrogenation of Ethanol Catalyzed by Pincer Ruthenium and Iron Complexes: Aliphatic Versus Aromatic Ligands. *ACS Catal.* **2013,** *3*, 2684-2688.

(27) Hou, C.; Zhang, Z.; Zhao, C.; Ke, Z. DFT Study of Acceptorless Alcohol Dehydrogenation Mediated by Ruthenium Pincer Complexes: Ligand Tautomerization Governing Metal Ligand Cooperation. *Inorg. Chem.* **2016,** *55*, 6539-6551.

(28) Le, L.; Liu, J.; He, T.; Malek, J. C.; Cervarich, T. N.; Buttner, J. C.; Pham, J.; Keith, J. M.; Chianese, A. R. Unexpected CNN-to-CC Ligand Rearrangement in Pincer–Ruthenium Precatalysts Leads to a Base-Free Catalyst for Ester Hydrogenation. *Organometallics* **2019,** *38*, 3311-3321.

(29) Addison, A. W.; Rao, T. N.; Reedijk, J.; van Rijn, J.; Verschoor, G. C. Synthesis, Structure, and Spectroscopic Properties of Copper(II) Compounds Containing Nitrogen–Sulphur Donor Ligands; the Crystal and Molecular Structure of Aqua[1,7-Bis(N-Methylbenzimidazol-2′-yl)-2,6-Dithiaheptane]Copper(II) Perchlorate. *J. Chem. Soc., Dalton. Trans.* **1984**, 1349-1356.

(30) The different rates of catalysis by RuCC-Et and RuCC-^{i}Pr are not easily explained, given the very similar rates of alkane evolution for the two catalysts. Work to develop quantitative kinetic models for these catalytic reactions is ongoing in our laboratory.

(31) Fogler, E.; Garg, J. A.; Hu, P.; Leitus, G.; Shimon, L. J. W.; Milstein, D. System with Potential Dual Modes of Metal–Ligand Cooperation: Highly Catalytically Active Pyridine-Based PNNH–Ru Pincer Complexes. *Chem. Eur. J.* **2014,** *20*, 15727-15731.

(32) (a) Takebayashi, S.; Bergens, S. H. Facile Bifunctional Addition of Lactones and Esters at Low Temperatures. The First Intermediates in Lactone/Ester Hydrogenations. *Organometallics* **2009,** *28*, 2349-2351. (b) Carpenter, I.; Eckelmann, S. C.; Kuntz, M. T.; Fuentes, J. A.; France, M. B.; Clarke, M. L. Convenient and Improved Protocols for the Hydrogenation of Esters Using Ru Catalysts Derived from (P,P), (P,N,N) and (P,N,O) Ligands. *Dalton Trans.* **2012,** *41*, 10136-10140. (c) Fuentes, J. A.; Smith, S. M.; Scharbert, M. T.; Carpenter, I.; Cordes, D. B.; Slawin, A. M. Z.; Clarke, M. L. On the Functional Group Tolerance of Ester Hydrogenation and Polyester Depolymerisation Catalysed by Ruthenium Complexes of Tridentate Aminophosphine Ligands. *Chem. Eur. J.* **2015,** *21*, 10851-10860. (d) Ogata, O.; Nakayama, Y.; Nara, H.; Fujiwhara, M.; Kayaki, Y. Atmospheric Hydrogenation of Esters Catalyzed by PNP-Ruthenium Complexes with an N-Heterocyclic Carbene Ligand. *Org. Lett.* **2016,** *18*, 3894-3897.

(33) (a) Kuriyama, W.; Ino, Y.; Ogata, O.; Sayo, N.; Saito, T. A Homogeneous Catalyst for Reduction of Optically Active Esters to the Corresponding Chiral Alcohols without Loss of Optical Purities. *Adv. Synth. Catal.* **2010,** *352*, 92-96. (b) Zhang, J.; Balaraman, E.; Leitus, G.; Milstein, D. Electron-Rich PNP- and PNN-Type Ruthenium(II) Hydrido Borohydride Pincer Complexes. Synthesis, Structure, and Catalytic Dehydrogenation of Alcohols and Hydrogenation of Esters. *Organometallics* **2011,** *30*, 5716-5724. (c) Spasyuk, D.; Smith, S.; Gusev, D. G. From Esters to Alcohols and Back with Ruthenium and Osmium Catalysts. *Angew. Chem. Int. Ed.* **2012,** *51*, 2772-2775. (d) Ziebart, C.; Jackstell, R.; Beller, M. Selective Catalytic Hydrogenation of Diethyl Oxalate and Related Esters. *ChemCatChem* **2013,** *5*, 3228-3231. (e) Chakraborty, S.; Dai, H.; Bhattacharya, P.; Fairweather, N. T.; Gibson, M. S.; Krause, J. A.; Guan, H. Iron-Based Catalysts for the Hydrogenation of Esters to Alcohols. *J. Am. Chem. Soc.* **2014,** *136*, 7869-7872. (f) vom Stein, T.; Meuresch, M.; Limper, D.; Schmitz, M.; Holscher, M.; Coetzee, J.; Cole-Hamilton, D. J.; Klankermayer, J.; Leitner, W. Highly Versatile Catalytic Hydrogenation of Carboxylic and Carbonic Acid Derivatives Using a Ru-Triphos Complex: Molecular Control over Selectivity and Substrate Scope. *J. Am. Chem. Soc.* **2014,** *136*, 13217-13225. (g) Korstanje, T. J.; van der Vlugt, J. I.; Elsevier, C. J.; de Bruin, B. Hydrogenation of Carboxylic Acids with a Homogeneous Cobalt Catalyst. *Science* **2015,** *350*, 298-302. (h) Brewster, T. P.; Rezayee, N. M.; Culakova, Z.; Sanford, M. S.; Goldberg, K. I. Base-Free Iridium-Catalyzed Hydrogenation of Esters and Lactones. *ACS Catal.* **2016,** *6*, 3113-3117. (i) Espinosa-Jalapa, N. A.; Nerush, A.; Shimon, L. J. W.; Leitus, G.; Avram, L.; Ben-David, Y.; Milstein, D. Manganese-Catalyzed Hydrogenation of Esters to Alcohols. *Chem. Eur. J.* **2017,** *23*, 5934-5938. (j) Yuwen, J.; Chakraborty, S.; Brennessel, W. W.; Jones, W. D. Additive-Free Cobalt-Catalyzed Hydrogenation of Esters to Alcohols. *ACS Catal.* **2017,** *7*, 3735-3740. (k) Anaby, A.; Schelwies, M.; Schwaben, J.; Rominger, F.; Hashmi, A. S. K.; Schaub, T. Study of Precatalyst Degradation Leading to the Discovery of a New Ru^{0} Precatalyst for Hydrogenation and Dehydrogenation. *Organometallics* **2018,** *37*, 2193-2201.

(34) Widegren, M. B.; Clarke, M. L. Manganese Catalyzed Hydrogenation of Enantiomerically Pure Esters. *Org. Lett.* **2018,** *20*, 2654-2658.

(35) Yang, X. H.; Yue, H. T.; Yu, N.; Li, Y. P.; Xie, J. H.; Zhou, Q. L. Iridium-Catalyzed Asymmetric Hydrogenation of Racemic Alpha-Substituted Lactones to Chiral Diols. *Chem. Sci.* **2017,** *8*, 1811-1814.

(36) Alberico, E.; Lennox, A. J.; Vogt, L. K.; Jiao, H.; Baumann, W.; Drexler, H. J.; Nielsen, M.; Spannenberg, A.; Checinski, M. P.; Junge, H.; Beller, M. Unravelling the Mechanism of Basic Aqueous Methanol Dehydrogenation Catalyzed by Ru-PNP Pincer Complexes. *J. Am. Chem. Soc.* **2016,** *138*, 14890-14904.

(37) (a) Dub, P. A.; Henson, N. J.; Martin, R. L.; Gordon, J. C. Unravelling the Mechanism of the Asymmetric Hydrogenation of Acetophenone by [RuX_2(Diphosphine)(1,2-Diamine)] Catalysts. *J. Am. Chem. Soc.* **2014,** *136*, 3505-3521. (b) Dub, P. A.; Gordon, J. C. The Mechanism of Enantioselective Ketone Reduction with Noyori and Noyori-Ikariya Bifunctional Catalysts. *Dalton Trans.* **2016,** *45*, 6756-6781. (c) Dub, P. A.; Scott, B. L.; Gordon, J. C. Why

Does Alkylation of the N-H Functionality within M/NH Bifunctional Noyori-Type Catalysts Lead to Turnover? *J. Am. Chem. Soc.* **2017,** *139*, 1245-1260.

(38) (a) Hu, P.; Fogler, E.; Diskin-Posner, Y.; Iron, M. A.; Milstein, D. A Novel Liquid Organic Hydrogen Carrier System Based on Catalytic Peptide Formation and Hydrogenation. *Nature Commun.* **2015,** *6*, 6859-6865. (b) Kumar, A.; Janes, T.; Espinosa-Jalapa, N. A.; Milstein, D. Selective Hydrogenation of Cyclic Imides to Diols and Amines and Its Application in the Development of a Liquid Organic Hydrogen Carrier. *J. Am. Chem. Soc.* **2018,** *140*, 7453-7457. (c) Xie, Y.; Hu, P.; Ben-David, Y.; Milstein, D. A Reversible Liquid Organic Hydrogen Carrier System Based on Methanol-Ethylenediamine and Ethylene Urea. *Angew. Chem. Int. Ed.* **2019,** *58*, 5105-5109.

(39) Kumar, A.; Janes, T.; Espinosa-Jalapa, N. A.; Milstein, D. Manganese Catalyzed Hydrogenation of Organic Carbonates to Methanol and Alcohols. *Angew. Chem. Int. Ed.* **2018,** *57*, 12076-12080.

(40) (a) Srimani, D.; Mukherjee, A.; Goldberg, A. F.; Leitus, G.; Diskin-Posner, Y.; Shimon, L. J.; Ben David, Y.; Milstein, D. Cobalt-Catalyzed Hydrogenation of Esters to Alcohols: Unexpected Reactivity Trend Indicates Ester Enolate Intermediacy. *Angew. Chem. Int. Ed.* **2015,** *54*, 12357-12360. (b) Daw, P.; Ben-David, Y.; Milstein, D. Direct Synthesis of Benzimidazoles by Dehydrogenative Coupling of Aromatic Diamines and Alcohols Catalyzed by Cobalt. *ACS Catal.* **2017,** *7*, 7456-7460.

(41) Tang, Z.; Otten, E.; Reek, J. N.; van der Vlugt, J. I.; de Bruin, B. Dynamic Ligand Reactivity in a Rhodium Pincer Complex. *Chem. Eur. J.* **2015,** *21*, 12683-12693.

(42) (a) Butschke, B.; Fillman, K. L.; Bendikov, T.; Shimon, L. J.; Diskin-Posner, Y.; Leitus, G.; Gorelsky, S. I.; Neidig, M. L.; Milstein, D. How Innocent Are Potentially Redox Non-Innocent Ligands? Electronic Structure and Metal Oxidation States in Iron-PNN Complexes as a Representative Case Study. *Inorg. Chem.* **2015,** *54*, 4909-4926. (b) Butschke, B.; Feller, M.; Diskin-Posner, Y.; Milstein, D. Ketone Hydrogenation Catalyzed by a New Iron(II)–PNN Complex. *Catal. Sci. Technol.* **2016,** *6*, 4428-4437. (c) Du, X.; Zhang, Y.; Peng, D.; Huang, Z. Base-Metal-Catalyzed Regiodivergent Alkene Hydrosilylations. *Angew. Chem. Int. Ed.* **2016,** *55*, 6671-6675. (d) Du, X.; Hou, W.; Zhang, Y.; Huang, Z. Pincer Cobalt Complex-Catalyzed Z-Selective Hydrosilylation of Terminal Alkynes. *Org. Chem. Front.* **2017,** *4*, 1517-1521. (e) Yang, Z.; Peng, D.; Du, X.; Huang, Z.; Ma, S. Identifying a Cobalt Catalyst for Highly Selective Hydrosilylation of Allenes. *Org. Chem. Front.* **2017,** *4*, 1829-1832.

(43) (a) Aparna, P. S.; Prabha, B.; Prakash, P.; Jijy, E.; Luxmi Varma, R.; Radhakrishnan, K. V. Ruthenium Catalyzed Desymmetrization of Diazabicyclic Olefins to Access Heteroaryl Substituted Cyclopentenes through C–H Activation of Phenylazoles. *Tetrahedron Lett.* **2014,** *55*, 865-868. (b) García-González, M. C.; Hernández-Vázquez, E.; Vengochea-Gómez, F. A.; Miranda, L. D. Palladium-Catalyzed Olefin Migration and 7-Endo - Trig Cyclization of Dehydroalanines. *Tetrahedron Lett.* **2018,** *59*, 848-852. (c) Kong, L.; Biletskyi, B.; Nuel, D.; Clavier, H. Cobalt(III)-Catalysed C–H Allylation with Vinylaziridines. *Org. Chem. Front.* **2018,** *5*, 1600-1603. (d) Tran, V. T.; Gurak, J. A., Jr.; Yang, K. S.; Engle, K. M. Activation of Diverse Carbon-Heteroatom and Carbon-Carbon Bonds Via Palladium(II)-Catalysed Beta-X Elimination. *Nature Chem.* **2018,** *10*, 1126-1133.

(44) Cope, A. C.; Foster, T. T.; Towle, P. H. Thermal Decomposition of Amine Oxides to Olefins and Dialkylhydroxylamines. *J. Am. Chem. Soc.* **1949,** *71*, 3929-3934.

(45) Macrae, C. F.; Edgington, P. R.; McCabe, P.; Pidcock, E.; Shields, G. P.; Taylor, R.; Towler, M.; van de Streek, J. Mercury: Visualization and Analysis of Crystal Structures. *J. Appl. Cryst.* **2006,** *39*, 453-457.

TOC Graphic:

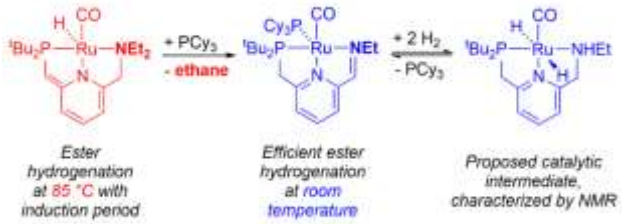
CO
H
tBu2P—Ru—NEt2
N
+ PCy3
- ethane
Cy3P
CO
tBu2P—Ru—NEt
N
+ 2 H2
- PCy3
CO
H
tBu2P—Ru—NHEt
N
H
Ester hydrogenation at 85 °C with induction period
Efficient ester hydrogenation at room temperature
Proposed catalytic intermediate, characterized by NMR